Study of Metal Transfer in Pulsed GMA Welding

Metal transfer is analyzed to determine optimum waveform for spatter free welding

BY S. UEGURI, K. HARA AND H. KOMURA

ABSTRACT. The metal transfer in pulsed GMA welding with mild steel electrode was investigated and the effect of the pulsed current on the transfer is discussed. The profile of the pendant droplet at the electrode tip was calculated by taking into account surface tension, gravity, and electromagnetic force, and was in good agreement with the image obtained by a high-speed movie camera. Also, the average heat content of droplets was obtained by calorimetry. As a result, the optimum pulse current form was clarified for spray transfer mode without spatter. With the pulse over a critical current, the electrode is heated to melt into a pendant droplet during the initial one third or two thirds of the pulse duration and remains as it is, despite the electromagnetic force. During the residual part of the duration, the pendant droplet is detached, being naturally superheated to 2100 °C (3812°F). When the pulse duration is too long beyond the optimum value, the molten electrode tip is prolonged, resulting in much spatter due to contact with the base metal.

Introduction

In GMA welding with Argon based shielding gas, the pendant droplet at the electrode tip is covered by the arc and becomes very small when the welding current is above a critical current. This transfer mode is called spray transfer, in which the droplet falls to the base metal without spattering and the arc behavior is well stabilized.

The object of pulsed GMA welding process is to realize the spray transfer mode at an average welding current below a critical value. The waveform should be made optimum to provide an equal-sized droplet from the electrode tip regularly per every pulse. It is difficult to control the waveform with conventional thyristors. Therefore, the optimum waveforms were produced by means of transistors capable of the fine control needed for the development of spatter-free, high quality welding.

In this paper, the metal transfer in pulsed GMA welding with mild steel electrode was studied: first, the variations of the transfer modes with various waveforms were observed by a high-speed movie camera; secondly, the profile of the pendant droplet at the electrode tip was calculated by assuming a static balance of forces on the droplet and compared with the experimental results; and finally, the significance of the optimum current waveform on the metal transfer was discussed in detail.

Paper selected by the Technical Papers Committee for presentation at the 64th annual AWS Convention in Philadelphia, Pa., April 24-29, 1983.

S. UEGURI, K. HARA and H. KOMURA are with the Product Development Laboratory of the Mitsubishi Electric Corporation, Amagasaki, Japan.

Experimental Procedure

Pulsed current supply

Figure 1 shows a schematic diagram of the pulsed current supply. The current is pulsated by the switching action of power transistors. The pulse parameters are shown in Fig. 2, where I_p denotes peak current, τ pulse duration and f pulse frequency. With this current supply, I_p, τ and f can be varied over a range of 300 ~ 550 A, 1 ~ 10 ms, and 30 ~ 500 Hz, respectively. The background current is about 50 A. The rising and falling rates

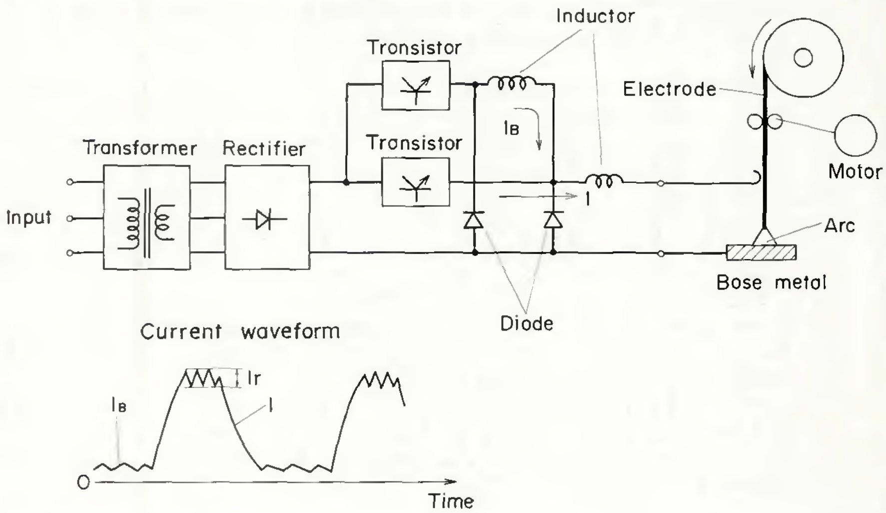

Fig. 1 — Schematic diagram of pulsed current supply

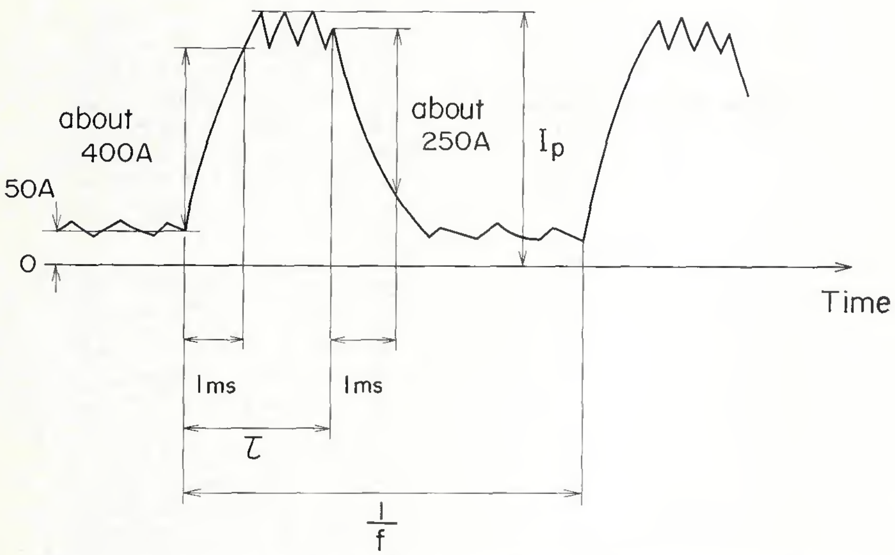

Fig. 2 — Pulse parameters: I_p is the peak current, τ is the pulse duration, and 1/f is one period

of the pulsed current are about 400 A/ms and 250 A/ms, respectively. The ripple current at the peak (I_r shown in Fig. 1) is about 80 A.

Materials

The electrode used was mild steel wire (AWS ER70S-G) with a diameter of 1.2 mm (0.047 in.). The base metal was mild steel plate of various dimensions. The shielding gas was composed of Ar (80%) and CO_2 (20%).

High-speed motion picture

Motion pictures of the welding arc and the droplet were taken by a high-speed movie camera (HYCAM 100, REDLAKE Co., Ltd.) at a speed of 3000 frames per second. The current waveform was also taken synchronously on the corresponding frame.

Average heat content

The experimental apparatus to measure the average heat content of droplets is shown in Fig. 3. The base metal was placed vertically and the electrode was positioned obliquely to it. The droplets fall through the slits into the copper basin of the calorimeter, resulting in the temperature rise of the surrounding water. The average heat content of droplets was calculated from the temperature rise and the weight of droplets collected in the copper basin. The error of measurement caused by the heat loss from the surrounding water was estimated to be within 7%.

Results

Optimum waveform of pulsed current

We observed the metal transfer modes with various current waveforms by means of the high-speed movie camera and classified them in terms of I_p and τ. The results are shown in Fig. 4 for an electrode feeding rate of 5 m/min (197 in./min) and an electrode extension of 15 mm (0.591 in.).

In the region (1), where I_p is smaller than 380 A which is the critical pulsed current with the mild steel electrode used in this experiment, the pendant droplet swells into a large globe independent of the pulse duration and the arc behavior becomes unstable accompanied by much spatter, since the electromagnetic force applied to the molten electrode tip is not directed to the base metal. In the region (2), where $I_p \geqq 380$ A and $\tau < \tau_{min}$, the pulse energy is too small to make a droplet transfer in one pulse and the pendant droplet swells into a large globe during several pulses. On the other hand, in the region (3), where $I_p \geqq 380$ A and $\tau_{min} \leqq \tau \leqq \tau_{max}$, one droplet with a diameter close to that of the electrode transfers regularly and reliably per every pulse; in this region, the arc behavior is extremely stabilized. Even if the arc length is shortened to the length twice the electrode diameter, the electrode seldom touches the base metal, so that spattering can be eliminated and high speed welding carried out. The pulsed current should be set in this optimum region (3). In the region (4), where

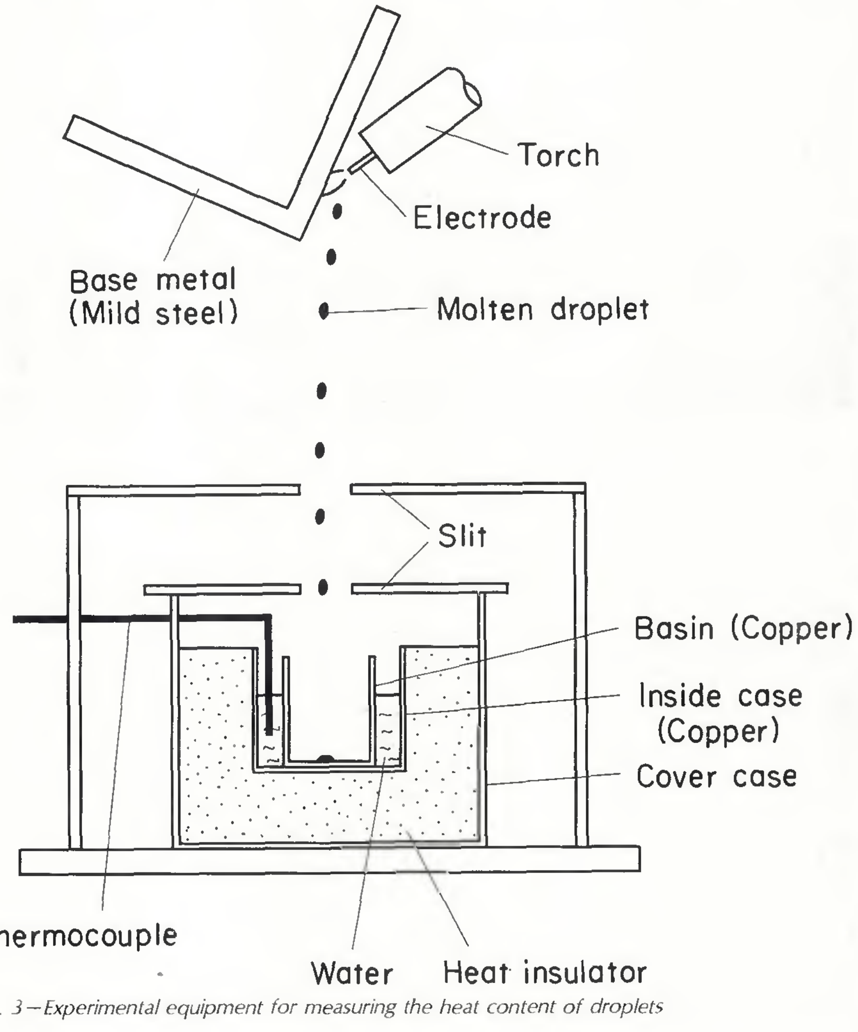

Fig. 3 — Experimental equipment for measuring the heat content of droplets

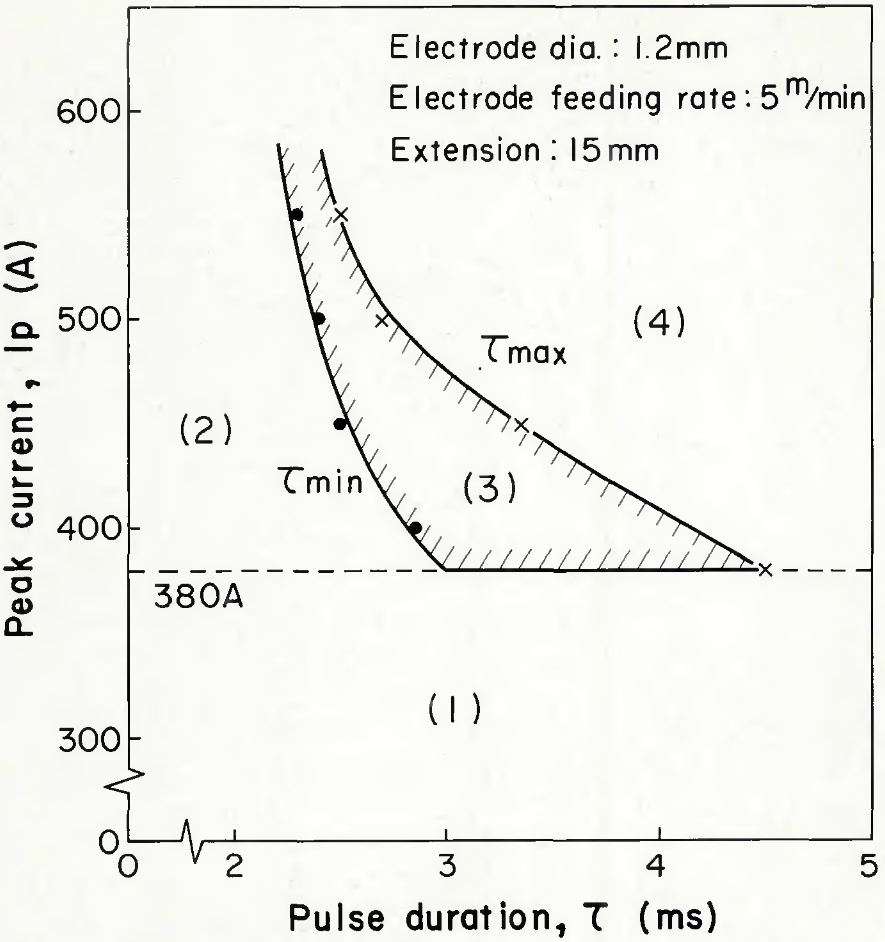

Fig. 4—Classified regions of metal transfer modes

$I_p > 380$ A and $\tau > \tau_{max}$, the transfer mode is apparently the spray type. However, the molten electrode tip is prolonged and touches the base metal causing much spatter. Furthermore, as τ increases in this region, f decreases at a constant feeding rate of electrode, resulting in incessant fluctuations of the arc length.

Comparison of spray mode between steady direct current and pulsed current

Figure 5 shows the time variations of the metal transfer observed with steady direct current above the critical steady current and Fig. 6, those observed with the pulsed current in the region (3). In the case of the steady direct current, a large amount of arc energy is continuously put into the electrode. Thus, the molten electrode tip tends to be prolonged, and the droplets transfer continuously, like streaming. On the other hand, in the case of the pulsed current, the droplets transfer intermittently like projectiles: the pendant droplet at the electrode tip is almost stationary and its shape is round until t_1, about 2.6 ms after the current rise. Then, the pendant droplet at the electrode tip is constricted, starts to fall and finally is detached from the electrode at t_2, about 2 ms after t_1. The remaining part of the pendant droplet restores the spherical shape during the background period after t_2.

Figure 7 shows the critical currents

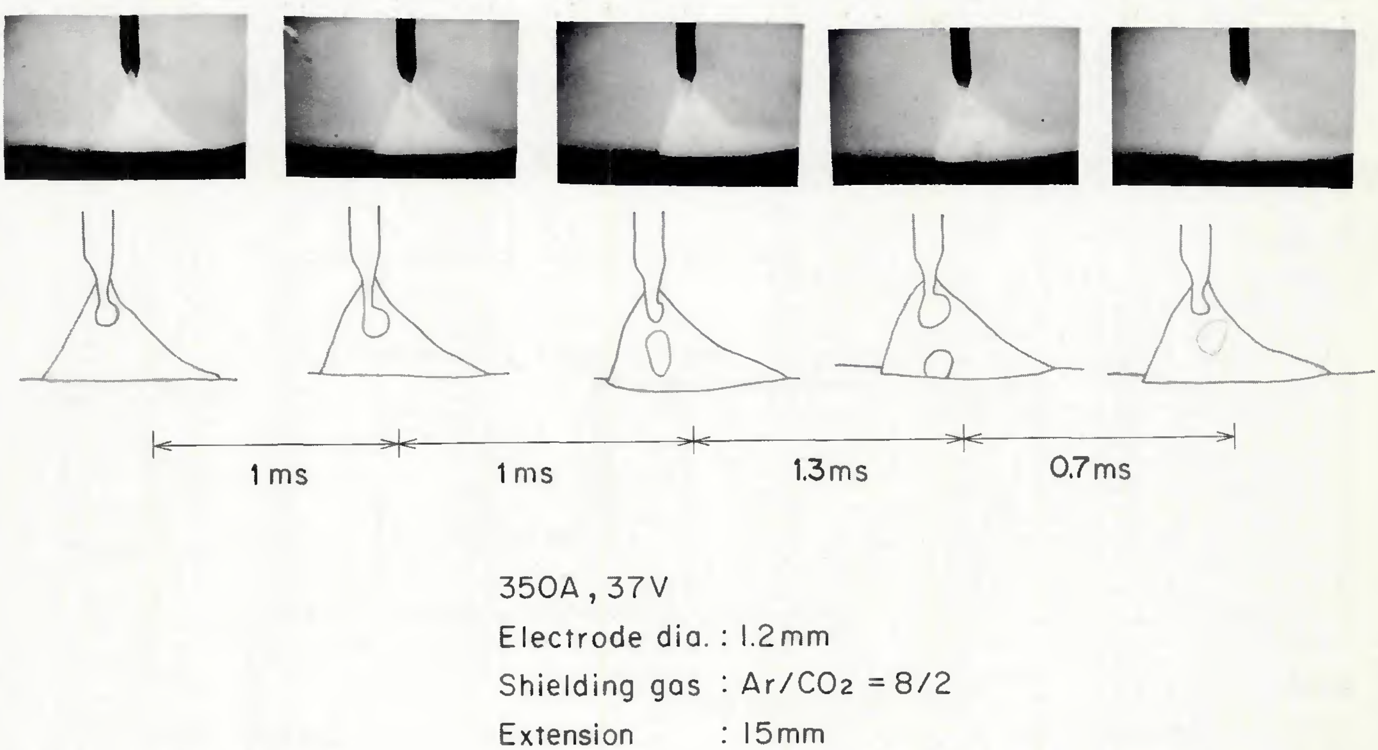

Fig. 5—Metal transfer with direct current

(pulsed and steady) as a function of the electrode diameter in both cases. It should be noted that higher currents are necessary with the pulsed current to realize the spray transfer. With the pulsed current, the pendant droplet is stationary at the end of the background period, so the additional current is required to overcome the drop inertia unlike the spray mode with the steady direct current which is in constant streaming motion once it is initiated.

Heat content of droplets

Figure 8 shows the average heat content, H_o in cal/g, of droplets measured at a wire feed rate of 5 m/min (197 in./min), and f of 125 Hz. When I_p is 380A, H_o is about 430 cal/g (1.95 × 10^5 cal/lb).

H_o is composed of the heat input both by the Joule heating, H_j, and arc heating, H_A. The mean value of the heat input by the arc, E_A in Watt, can be assumed to be proportional to the mean value of the welding current, I in A;

$E_A = \phi \cdot I$,

where ϕ is the equivalent melting voltage in V. I is defined as

$$\frac{1}{T}\int_{\text{one cycle}} i(t)\,dt,$$

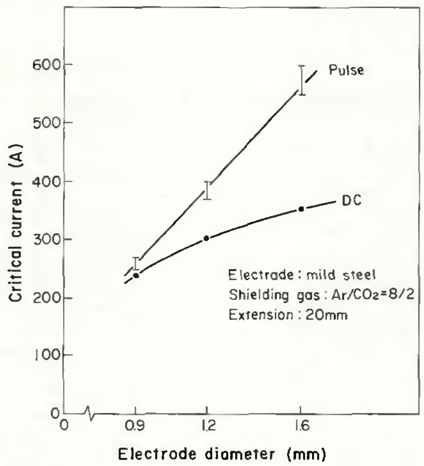

Fig. 7 — Critical currents for direct and pulsed current

where T is one period and is equal to 1/f, and i(t) is an instantaneous value of welding current.

According to Halmoy (Ref. 1), H_j is a function of $(I_{rms}/S)^2$ l/v, where S is the cross section of electrode, l the electrode extension, v the electrode feeding rate, and I_{rms} the effective current defined as

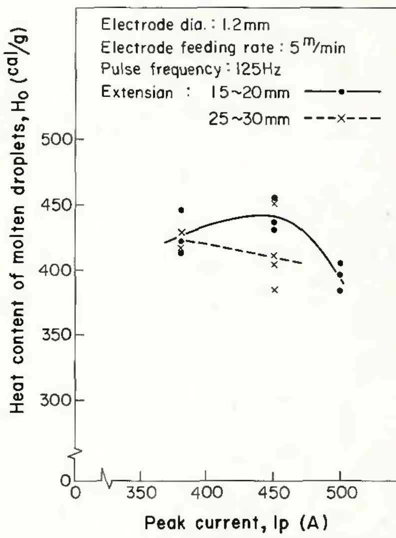

Fig. 8 — Heat content of molten droplets

$$\sqrt{\frac{1}{T}\int_{\text{one cycle}} i^2(t)\,dt}\ .$$

Figure 9 shows the relation between H_j and $(I_{rms}/S)^2$l/v for the mild steel electrode used in this study.

Once the values of H_o, l and I_{rms} are measured for given values of S, l and v, H_j

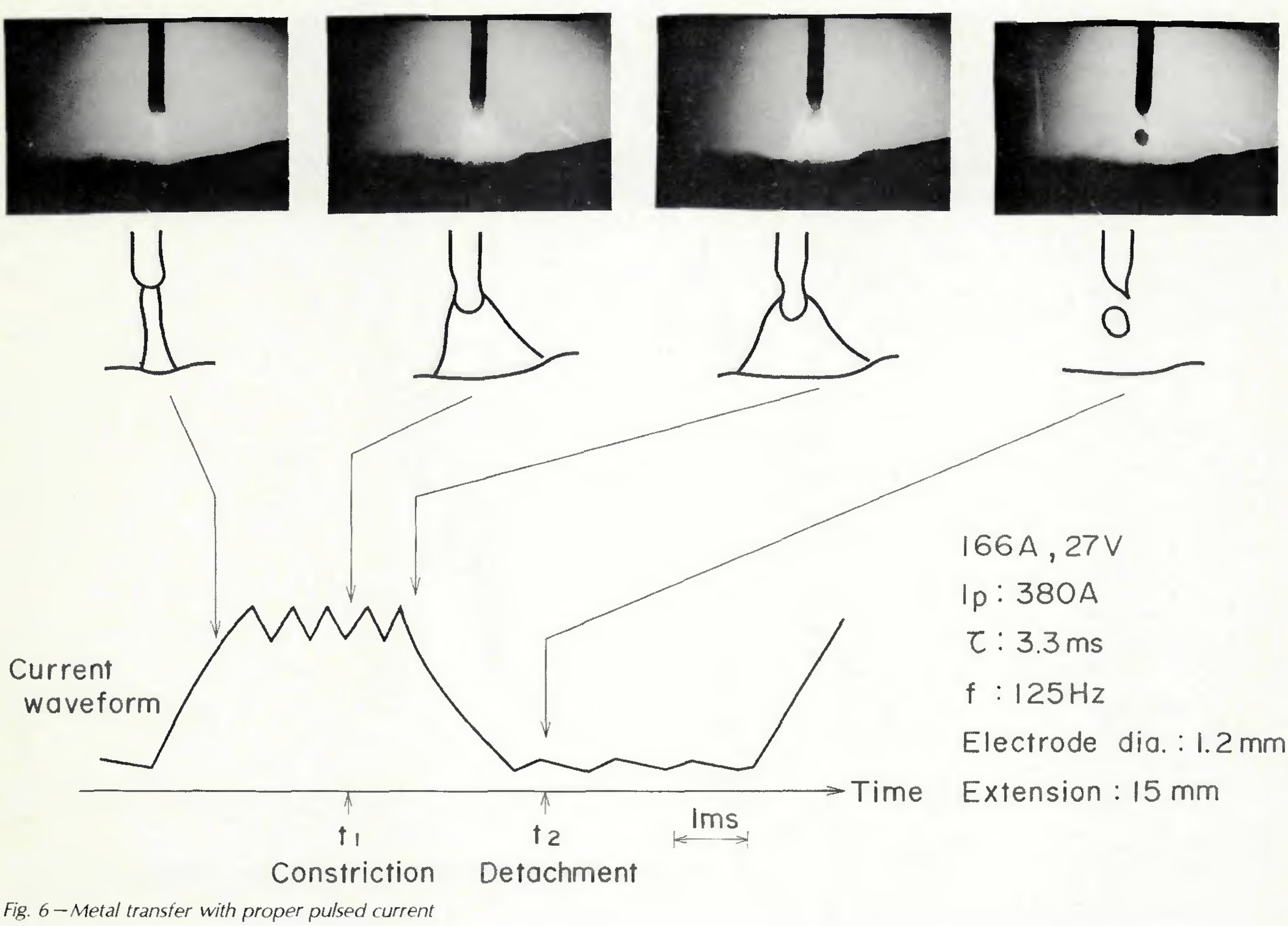

Fig. 6 — Metal transfer with proper pulsed current

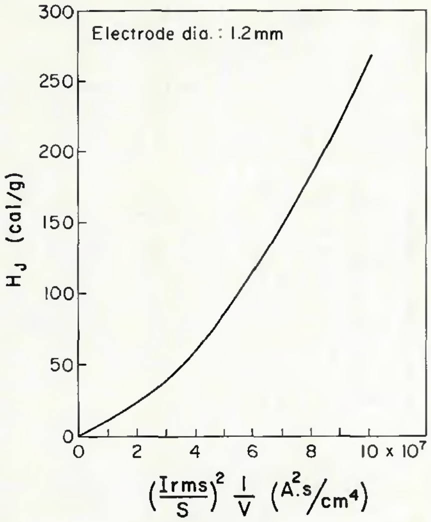

Fig. 9—Plot of H_j vs. $(I_{rms}/S)^2 \cdot l/v$

can be obtained from the relation in Fig. 9. And H_A can be obtained, since H_A is equal to H_o-H_j. The value of ϕ can also be calculated as follows,

$$\phi = \frac{E_A}{I} = \frac{4.2\ H_A\ \rho_t\ v\ S}{I} \quad (1)$$

where ρ_t is the density of electrode, 7.8 g/cm^3, and ρ_t vS expresses the weight of the electrode melted per second in g/s.

Now, we evaluate ϕ in order to discuss later the physical meaning of the pulsed current waveform. For example, when l = 15 mm = 1.5 cm, v = 5 m/min = 8.33 cm/s, I = 167 A, I_{rms} = 208 A and H_o = 430 cal/g,

$$(I_{rms}/S)^2 l/v = 6.22 \times 10^7\ A^2 \cdot s/cm^4.$$

From Fig. 9, H_j can be estimated to be 117 cal/g. Thus, H_A = 313 cal/g (1.42×10^5 cal/lb) and ϕ can be calculated to be 5.8 V.

Discussion

The optimum waveform of the pulsed current has been shown by the region (3) of Fig. 4. At a constant wire feed speed, a large value of f is preferable for practical use, because the frequency of metal transfer increases and the weld bead becomes uniform, the fluctuation of arc length caused by the metal transfer becomes little if any, and the arc length can be set so short without spatter that the welding speed can be increased. Therefore, we will study the physical meaning of the minimum pulse duration, τ_{min}, of the region (3). We will calculate the maximum weight of the pendant droplet and compare it with the experimental value at t_1 (Fig. 6), and we will discuss the time relation between the current waveform and the metal transfer phenomena.

Profile of pendant droplet

In the metal transfer by the pulsed current, it can be pointed out that the electrode melts gently, as shown in Fig. 6. We calculated the profile and the weight of the pendant droplet by using the equation of static balance of pressure. The definition of axes is shown in Fig. 10. Assuming that the density of the shielding gas is negligible compared with that of the pendant droplet and that the pendant droplet is a sphere at Z = 0 with a radius of b, the equation for the balance of pressure at $z = z_o$ can be written as follows (Ref. 2):

$$T\left(\frac{1}{R_1} + \frac{1}{R_2}\right) = \frac{2T}{b} - \rho_t g z_o \quad (2)$$

where T is the surface tension, R_1 the radius of inscribed sphere, R_2 the radius of curvature in the profile plane and g the gravitational acceleration. The solutions of equation (2) are illustrated in Fig. 11. The profile of the pendant droplet can be

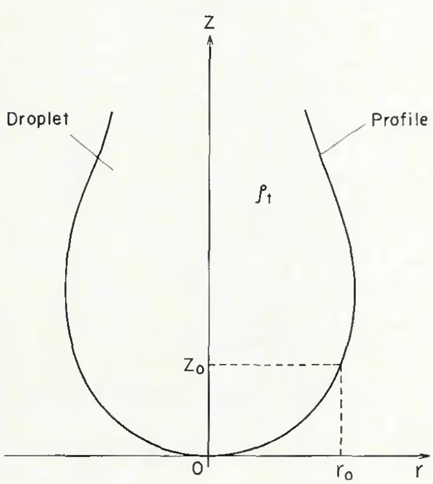

Fig. 10—Definition of axes: The point 0 is tip of the droplet, z is the center axis, ρ_t is the density of the droplet, and (r_0, Z_0) is the location of a point on the profile

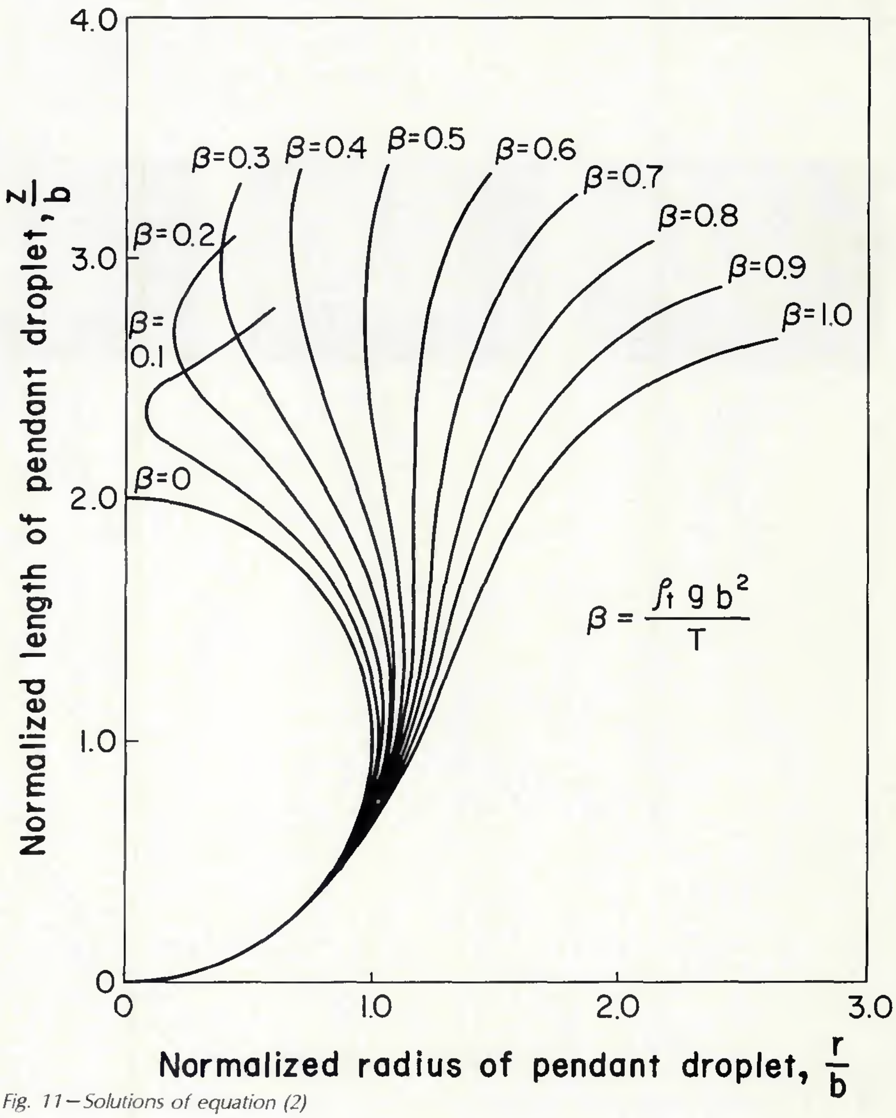

Fig. 11—Solutions of equation (2)

obtained by solving equation (2) on the assumption that r = R (R; radius of electrode) at the electrode tip and that the profile at the start of falling-off is equal to that enclosing the maximum volume.

Surface tension of pendant droplet

In order to estimate the surface tension of pendant droplets, we heated the electrode gently with a tungsten arc using a shielding gas of $80Ar/20CO_2$ as shown in Fig. 12. The electrode melts into a molten globe which, increasing its volume, falls off finally. The observed profile at the instant of falling off agreed well with the calculated one for a surface tension of 1200 dyn/cm (6.89×10^{-3} lb-force/in.), as shown in Fig. 12. This value will be used below in the estimation of the volume of pendant droplet.

Electromagnetic pinch force

Greene (Ref. 3) estimated the z-component, F in dyn, of the electromagnetic force by equation (3), assuming that the shape of the pendant droplet is a sphere and the arc current pours out at a uniform density from the hatched area of Fig. 13.

$$F = I^2 \left[\log \frac{\sin\Theta}{\sin\alpha} - \left(\frac{1}{4} + \frac{1}{1-\cos\Theta}\right) + \frac{2}{(1-\cos\Theta)^2} \log \frac{2}{1+\cos\Theta}\right], \quad (3)$$

where the dimension of I is e.m.u. Since this force is added to the gravity, ρ_t in equation (2) must be replaced by ρ_{total}, the effective mass reinforced by the pinch force.

Figure 14 shows the relation between ρ_{total}/ρ_t and the maximum weight of the pendant droplet, W, which was estimated by integrating equation (2) for 2R = 1.2 mm (4.73×10^{-2} in.), $\rho_t = 7.8$ g/cm^3 (0.0282 lb mass/in.^{3}), and T = 1200 dyn/cm (6.89×10^{-3} lb-force/in.). Without the pinch force (i.e., at $\rho_{total}/\rho_t = 1$) W is 370 mg. However, with the help of powerful pinch force, W decreases below 10 mg (0.022 lb).

When I and the current density are given, ρ_{total} can be estimated by equation (3). The relation between W and I can be obtained by the value of W at this ρ_{total} in Fig. 14. This relation is shown in Fig. 15. The parameter N in Fig. 15 is defined by

$$N = (I/A)^2 R^3/T,$$

where A is the hatched area of Fig. 13. The weight of the pendant droplet reaches the minimum, W_c, when the arc covers the pendant droplet and Θ is equal to α. This is the boundary between the globular and the spray transfer. The minimum weight, W_c, and the critical current, I_c, (i.e., the current at W_c) are expressed in terms of N in Fig. 16. When the current density increases as with CO_2 rich shielding gas, I_c increases remarkably, though W_c decreases.

In order to compare the practical weight of the pendant droplet with W_c, we apply the pulsed critical current of 380 A for 1.2 mm (0.047 in.) diameter electrode to the curves in Fig. 16. Thus, we can estimate N to be 0.18 for a shielding gas of 80 Ar/20 CO_2 and an electrode diameter of 1.2 mm (0.047 in.), which leads to the average current density of 10^4 A/cm^2 (6.45×10^4 A/in.^{2}), and W_c of 7.3 mg (1.61×10^{-5} lb). It is concluded that, from the viewpoint of the static balance, the pendant droplet starts to fall off just when its weight exceeds 7.3 mg under the peak current of 380 A. The weight of the pendant droplet at the electrode tip at the time t_1 in Fig. 6 was estimated from the enlarged photograph of the high-speed motion picture to be about 8 mg. Thus, it is reasonable to conclude that t_1 is the time when the weight of the pendant droplet exceeds 7.3 mg (1.76×10^{-5} lb).

As mentioned before, the transfer phenomena are different between the steady direct current and the pulsed current. With the pulsed current, the pendant droplet at the electrode tip is almost stationary until it is constricted and starts to fall. But with the steady direct current, the droplet is streaming towards the base metal. So, the profile and the volume of the pendant droplet at the electrode tip with the pulsed current can be calculated by the equation of the static pressure balance. The "static" pressure balance cannot be applied to the spray mode with the steady direct current. Greene developed his theory (Ref. 3) on the assumption of the static pressure balance. He did not make clear in what current waveform the "static" condition held good. We made clear that the "static" condition did hold good in the droplet transfer phenomena with the pulsed current.

Significance of current waveform

After the pendant droplet is constricted, it falls off being covered by the arc. The current should be kept at the peak value still after t_1 to exercise its electromagnetic force over the droplet. If the current falls down just after t_1, the electromagnetic pinch force decreases and the pendant droplet never transfers, which is an example of the region (2) of Fig. 4.

After t_1, the constricted portion of the pendant droplet gradually becomes thin and the arc covers only the falling droplet. As the current must be kept high after t_1, the droplet is forced to be superheated much higher than the melting point of 1535 °C (2795 °F) and its heat content, H_o, increases to about 430 cal/g (2100 °C).

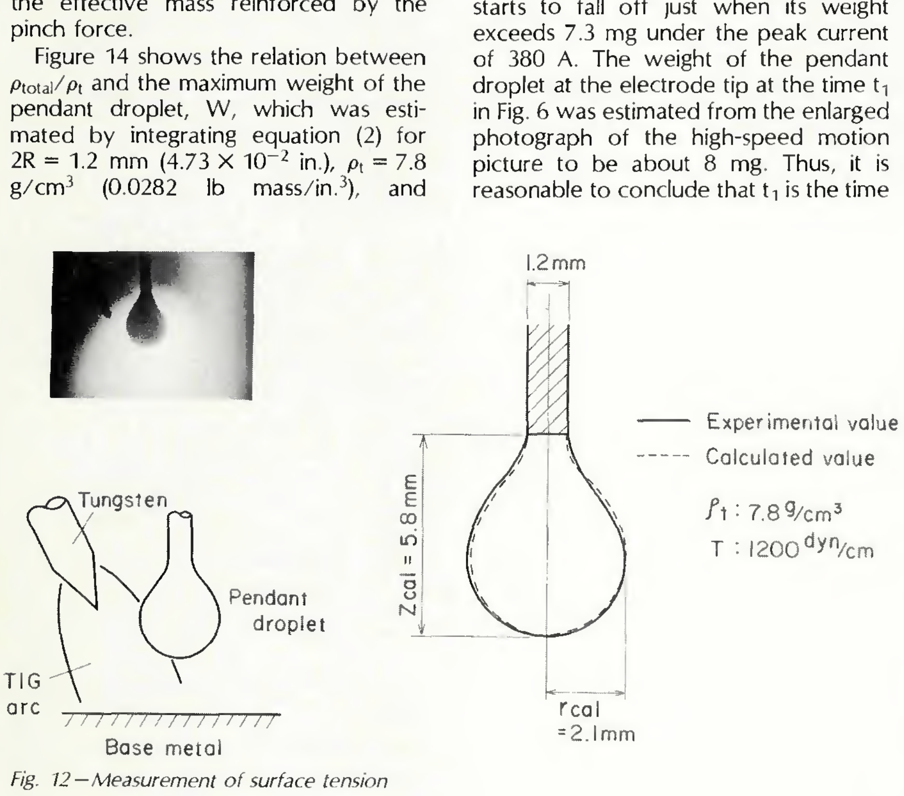

Fig. 12 — Measurement of surface tension

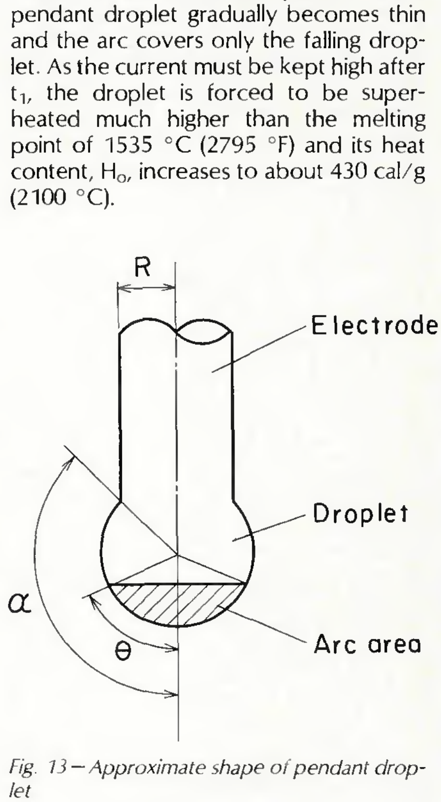

Fig. 13 — Approximate shape of pendant droplet

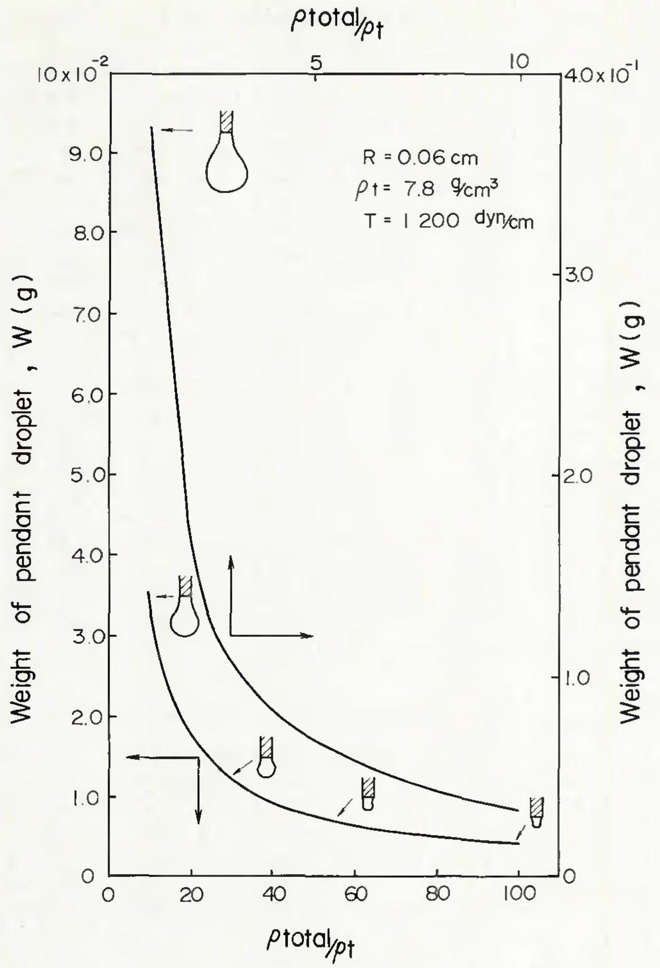

Fig. 14 — Relation between ρ_{total}/ρ_t and W

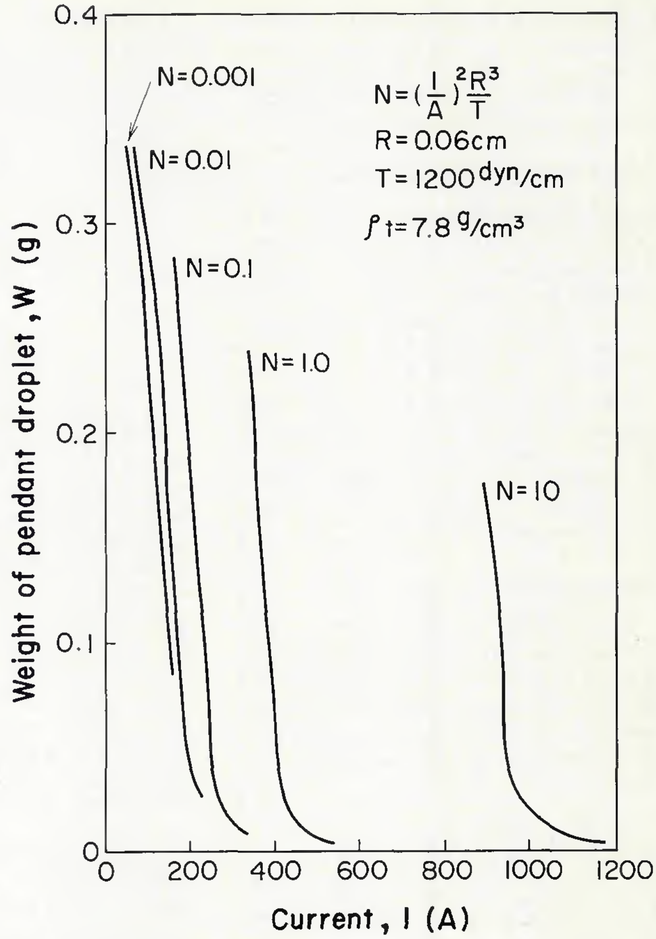

Fig. 15 — Relation between W and I

We estimate the average heat content, H_1, of the pendant droplet at t_1 from H_o (430 cal/g), ϕ and the current waveform from t_1 to t_2 ($\int_{t_1}^{t_2} i(t) = 0.583$ A · s) for the following conditions:

Wire feed: 5 m/min (197 in./min)

Pulse frequency : 125 Hz

Peak current : 380 A

The value of ϕ was estimated previously to be 5.8 V. From the same derivation in other conditions of I_p (380 ~ 500 A), l(10 ~ 30 mm) and v (5 ~ 9 m/min), the mean value of ϕ was estimated to be 6.0 V. So, in the discussion hereafter, we will adopt 6.0 V for the value of ϕ.

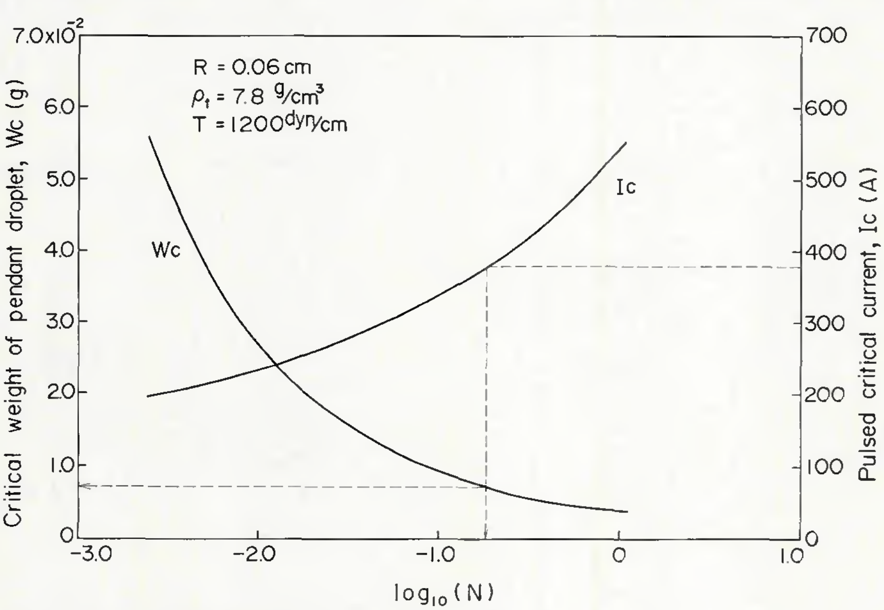

Fig. 16 — Relation between W_c and I_c

The electrode feed rate is 5 m/min, that is 735 mg/s, and the pulse frequency is 125 Hz. As one droplet is transferred per every pulse, the average mass of falling droplet is

$$\frac{735\ [\text{mg/s}]}{125\ [\text{Hz}]} = 5.88\ [\text{mg}].$$

The derivation of H_1 is as follows:

The heat input to the constricted droplet (5.88 mg) from t_1 to t_2:

$$0.583\ [\text{A} \cdot \text{s}] \times 6.0\ [\text{V}] \times \frac{1}{4.2\ [\text{J/cal}]} = 0.833\ [\text{cal}]$$

The heat input per unit mass, ΔH_1:

$$\frac{0.833\ [\text{cal}]}{5.88\ [\text{mg}]} = 142\ [\text{cal/g}]$$

The average heat content of droplets at t_1, H_1:

$H_1 = H_o - \Delta H_1 = 288$ [cal/g] (1.31×10^5 [cal/lb]).

This value of H_1 is nearly equal to 300 cal/g which is the heat content of molten steel at the melting point. At t_1, the pendant droplet has a weight of W_c and a temperature of about melting point. Table 1 shows ΔH_1 and H_1 derived as mentioned above for several cases.

The electrode is heated by the next pulse during the period from the detachment of a droplet to the constriction of the following droplet. From the current waveform during this period, we can estimate the heat input, ΔH_2, to the electrode by the arc, as follows,

$$0.798[A \cdot s] \times 6.0[V] \times \frac{1}{4.2\ [J/cal]} = 1.14\ [cal/one\ droplet].$$

This corresponds to 194 cal/g. The pendant droplet receives also the heat input of 117 cal/g by the Joule heating at the 15 mm extension. Thus, the whole heat content of the droplet at t_1 is 311 cal/g (1.41×10^5 cal/lb). This shows again that the temperature of pendant droplet at t_1 is nearly equal to the melting point. ΔH_2 and H_j for several cases are also shown in Table 1. Figure 17 shows the time relation described above among the heat content of droplets, the current waveform, and the mode of metal transfer. The optimum pulse duration is divided at time t_1 into two parts, "the melting period" and "the detaching period."

If the pulse duration lasts long beyond t_2, the electrode is heated to melt excessively by the arc before the droplet falls away and the following droplets begin to transfer during the same pulse period: this is the case with the region (4) of Fig. 4 and the beginning of steady current.

Table 1—Analysis of Heat Content of Droplets

Peak current (A)	Electrode extension (mm)	H_o observed (cal/g)	ΔH_1 calculated (cal/g)	$H_1 = H_o - \Delta H_1$ (cal/g)	ΔH_2 calculated (cal/g)	H_j calculated (cal/g)	$H_j + \Delta H_2$ (cal/g)
380	15	430	142	288	194	117	311
450	15	440	158	282	163	131	294
500	15	400	95	305	207	119	326
450	30	410	91	319	157	161	318

1. Electrode dia. : 1.2 mm
2. Electrode feeding rate : 5 m/min
3. Pulse frequency : 125 H_z

Weld sample

We have developed a transistor-controlled arc welding machine which utilizes the pulsed current having I_p and τ in the region (3) of Fig. 4. The pulse frequency is automatically linked to the manually-set electrode feed rate, and the region (3) is automatically attained by electronic circuitry. The arc length is kept constant during the welding operation, independent of small fluctuations of electrode extension, since the arc voltage is continuously monitored and adjusted to the proper value by the control of pulse duration. Spatter-free stable beads can be obtained with this welding machine, as shown in Fig. 18 in which the bead is compared to a conventional GMA weld with CO_2 shielding gas.

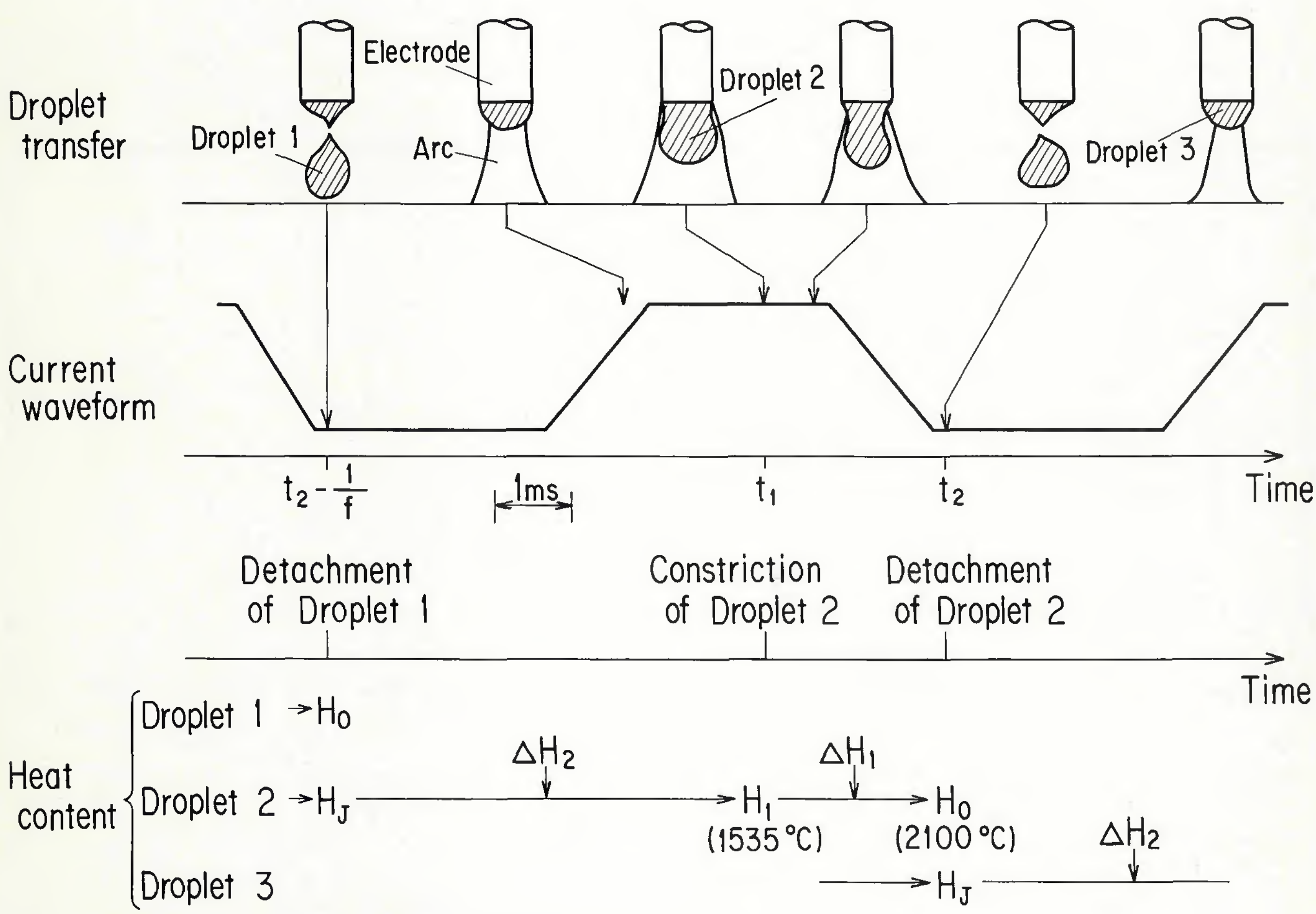

Fig. 17—Time relation among current waveform, metal transfer and heat content

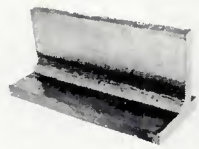

(A) CONVENTIONAL GMA WELDING
(SHIELDING GAS : CO_2)

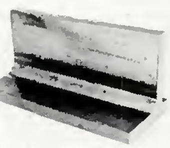

(B) PULSED GMA WELDING
(SHIELDING GAS : Ar/CO_2=8/2)
BASE METAL : 9mm(0.355in) MILD STEEL
WELDING CURRENT : 250A
WELDING SPEED : 420mm/min
(165in/min)

Fig. 18 — Weld bead samples

Conclusions

In pulsed GMA welding, I_p should be set above the critical current and τ should be so adjusted that the electrode tip is melted in proper size and a droplet transferred reliably per every pulse to the base metal.

At the time of t_1, when the pendant droplet is constricted and starts to fall, its weight is nearly equal to the maximum weight of the pendant droplet that can attach to the electrode tip, and its temperature is nearly equal to the melting point. After t_1, the current should be kept at the peak value to detach perfectly the pendant droplet from the electrode tip, so the droplet is forced to be superheated up to about 2100 °C (3812 °F). If the pulse duration lasts beyond t_2, the volume of molten electrode increases and the following droplets fall down. If the pulse duration is too short, a pendant droplet can not be detached in every pulse.

The optimum pulse duration is divided at time t_1 into two parts, "the melting period" and "the detaching period."

The pendant droplet is gently melted at the electrode tip in the case of the spray transfer under the pulsed current. On the other hand, the molten electrode tip is prolonged and droplets fall in a streaming manner under the direct current.

The critical current of the pulsed current is larger than that of the direct current.

Greene assumed that the pendant droplet at the electrode tip was spherical and stood still until it started to fall and calculated the volume of the pendant droplet at the electrode tip. But he never made clear in what case his assumption was correct. We have made clear by experiment that his assumption is correct for the spray transfer mode with the pulsed current.

Acknowledgements

The authors wish to express their appreciation to Mr. J. Ukai and Mr. T. Mizuno for their useful suggestions, and to Mr. Y. Tabata for his comment and help in the experiment.

References

1. Halmoy, E. 1979. Wire melting rate, droplet temperature, and effective anode melting potential. *Conference on Arc Physics and Weld Pool Behavior*, pp. 49-57.
2. Matijević, E. 1969. *Surface and Colloid Science* 2 (2). New York, John Wiley & Sons.
3. Greene, W.J. 1960. An analysis of transfer in gas-shielded welding arcs. *Trans. A.I.E.E.* 79: 194-203.

Correction

In the appendix of the paper, "Adaptive Welding by Fiber Optic Thermographic Sensing: An Analysis of Thermal and Instrumental Considerations," by J. P. Boillot, P. Cielo, G. Bégin, C. Michel, M. Lessard, P. Fafard, and D. Villemure, which appeared in the July 1985 *Welding Journal*, the Greek character delta (δ) was inadvertently substituted for the mathematical sign of partiality (∂). The corrected equations follow:

$$\frac{\partial T}{\partial t} = \partial\left[\frac{\partial^2 T}{\partial x^2} + \frac{\partial^2 T}{\partial y^2} + \frac{\partial^2 T}{\partial z^2}\right] \quad \text{(A-1)}$$

$$\rho s\, Cp \frac{\partial T}{\partial t} = -\,\text{div}\, \underline{Q} \quad \text{(A-3)}$$

$$\frac{\partial T}{T \partial x} = \text{constant} \quad \text{(A-5)}$$

$$\frac{\partial \sigma}{\partial T}\frac{\partial T}{\partial x} = \mu \frac{v}{\ell} \quad \text{(A-6)}$$

$$v = \frac{K}{\mu}\frac{\partial T}{\partial x} \quad \text{(A-7)}$$